A Letters Journal Exploring
the Frontiers of Physics

OFFPRINT

2D foam coarsening in a microfluidic system

J. Marchalot, J. Lambert, I. Cantat, P. Tabeling and M.-C. Jullien

EPL, **83** (2008) 64006

http://www.epljournal.org
epl
A Letters Journal Exploring the Frontiers of Physics
Athens login
Switch to test
IOP login:
Password:
Go
Create account | Alerts | Contact us
Journals Home
Journals List
This Journal
Search
Authors
Referees
Librarians
User Options
Help
This Journal
Partners
Editorial information
Editorial & Advisory Boards
Abstracted in
Request sample copy
For authors
For referees
For co-editors
Pricing & ordering
Events calendar
Copyright & permissions
info@epljournal.org
recommend this journal
e-mail alerts
An easy way to keep up to date
RSS
RSS feed: latest articles
About RSS
Done

A Letters Journal Exploring
the Frontiers of Physics

September 2008

EPL, **83** (2008) 64006
doi: 10.1209/0295-5075/83/64006

www.epljournal.org

2D foam coarsening in a microfluidic system

J. Marchalot[1], J. Lambert[2], I. Cantat[2], P. Tabeling[3] and M.-C. Jullien[1]

[1] *SATIE, ENS Cachan Bretagne, CNRS, UEB - av Robert Schuman, F-35170 Bruz, France, EU*
[2] *IPR, CNRS UMR 6251, Université de Rennes 1 - Campus Beaulieu, F-35042 Rennes Cedex, France, EU*
[3] *MMN, CNRS UMR 7083, ESPCI - 10 rue Vauquelin, F-75005 Paris, France, EU*

received 13 February 2008; accepted in final form 6 August 2008

PACS `47.57.Bc` – Foams and emulsions
PACS `66.10.C-` – Diffusion and thermal diffusion
PACS `81.40.Cd` – Solid solution hardening, precipitation hardening, and dispersion hardening; aging

Abstract – We report an experimental study of 2D microfoam coarsening confined in a micrometer scale geometry, the typical bubbles diameter being of the order of 50–100 μm. These experiments raise both fundamental and applicative issues. For applicative issues: what is the typical time of foam ageing (for a polydisperse foam) in microsystems in scope of gas pocket storage in lab-on-a-chips? Experimental results show that a typical time of 2–3 mn is found, leading to the possibility of short-time storing, depending on the application. For fundamental interests, 2D foam ageing is generally described by von Neumann's law (von Neumann J., *Metal Interfaces* (American Society of Metals, Cleveland) 1952, p. 108) which is based on the hypothesis that bubbles are separated by thin films. Does this hypothesis still hold for foams confined in a 40 μm height geometry? This problematic is analyzed and it is shown that von Neumann's law still holds but that the diffusion coefficient involved in this law is modified by the confinement which imposes a curvature radius at Plateau borders. More precisely, it is shown that the liquid fraction is high on a film cross-section, in contrast with macrometric experiments where drainage occurs. An analytical description of the diffusion is developped taking into account the fact that soap film height is only a fraction of the cell height. While most of microfoams are flowing, the experimental set-up we describe leads to the achievement of a motionless confined microfoam.

Introduction. – Microfluidics is on the way to be one of the most stimulating research field for chemical, medical and pharmaceutical industries. In this paper we study the static evolution of a multiphase flow (a foam) in a microfluidic system. Multiphase flows occur in many processes and are very promising for biotechnologies and especially for their applications in a lab-on-chip setting. They may be used, for example, for the storage of gas micropockets or for amphiphilic molecules transport (like proteins which generally adsorb on the walls when there is only one liquid phase [1,2]). For these purposes, the time scale associated to foam coarsening is crucial. As the 3D foam coarsening process significantly differs from the 2D one, the average coarsening time scale obtained for a 3D microfoam [3,4] does not directly apply in confined geometries. The study of 2D dry foams has been largely analyzed both theoretically and experimentally (see [5] for a review) since Plateau's first experiments in 1873. At millimetric scale or above, there is a general agreement between theory and experiments for foam ageing, which is essentially governed by von Neumann's law [6,7], but, to our best knowledge, nothing has been reported in this field for 2D microfoams. Von Neumann's law includes the hypothesis that bubbles are separated by a thin film; due to confinement, the foam structure is modified and one can ask if the macroscopic law still holds.

Most of the papers dealing with microfoams in 2D devices, focuses on flowing microfoams [8,9]. In this paper, we show that it is possible to build experiments on motionless microfoams, allowing for ageing studies. Typical sample contains about 100 bubbles at the initial time, some of which touch the boundary of the container. Boundary effects are therefore carefully discussed. We determine the order of magnitude of coarsening time scale, which is directly useful for applications, and we also define a statiscally stationary regime at first 10 mn. We re-establish von Neumann's law for the specific foam structure encountered in microchannels and we show that the confinement has an important effect on the effective diffusion coefficient.

2D foam coarsening in macrosystems. – In the case of a two-dimensional unbounded dry foam, the analysis can be based on von Neumann's law, for each individual cell of area A and number of sides n:

$$\frac{\mathrm{d}A}{\mathrm{d}t} = D_{\text{eff}}(n-6). \tag{1}$$

The effective diffusion coefficient D_{eff} is related to k, the permeability constant of the films which separate bubbles, and to γ, the surface tension of a single interface, through the equation [10]

$$D_{\text{eff}} = \frac{2\pi}{3}\frac{\gamma\, k}{P^0}. \tag{2}$$

Here P^0 is the average pressure in the gas. The local volume flux of gas through a film of area A, submitted to a pressure difference ΔP is given by

$$\mathrm{d}V/\mathrm{d}t = kA\Delta P/P^0. \tag{3}$$

von Neumann's equation is accurate for inner bubbles in a 2D foam [11], *i.e.* for bubbles that are surrounded by other bubbles (no contact with lateral walls). In the case of a foam confined by walls, this law has to be adjusted, due to the fact that two types of bubbles have to be considered: peripheral or edge bubbles (E-bubbles) and inner bubbles (I-bubbles). Rosa and Fortes proposed a model with modified equations for E-bubbles [12]. In the following study, statistics will be specified on I-bubbles, while it has been previously checked that E-bubbles evolve as expected.

Macrofoam vs. microfoam. – First, due to a large surface/volume ratio, volumic forces are negligible compared to surface forces. This leads to the absence of vertical drainage (due to gravity) on such small length scales. Note that Stavans [13] found good agreement with von Neumann's law while Plateau borders are kept nearly constant and thin at all times, *i.e.* for a drained foam.

Radii of curvature are smaller due to confinement so pressures and pressure differences are much higher than in macrofoam. Surprisingly, von Neumann's law (eq. (1)) shows that this is without direct influence on the coarsening rate, which only depends on the foam topology. Nevertheless, this law assumes that a thin film between two bubbles adopts a cylindrical shape (without curvature in a plane perpendicular to the plates) and that the menisci along its contact with each plates (called *Plateau borders*) are of negligible thickness (see fig. 1c). This is usually verified in macroscopic 2D dry foams, but is *a priori* wrong at microscale, as discussed in the next part: top and bottom Plateau borders are very close, if not in contact. Finally, the coarsening rate is strongly influenced by the film thickness through the permeability k. This thickness, of the order of 10–30 nanometers, depends on the pressure difference between the liquid phase and the gas phase, and is probably very thin in microscopic situations.

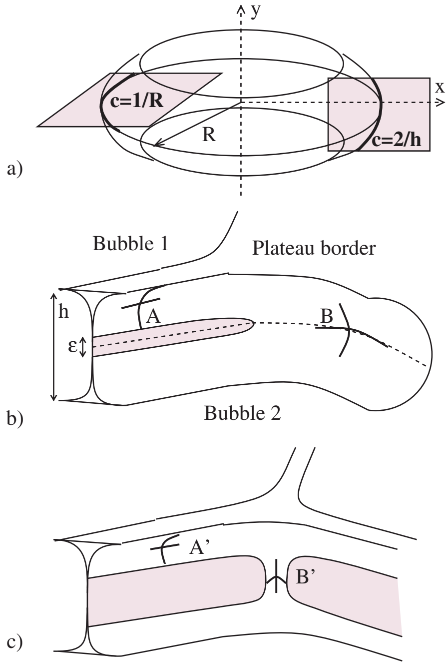

Fig. 1: Bubble shape between 2 plates for various liquid fractions. The value of the principal curvature is estimated in the text. (a) Wet limit: no contact between the bubbles. (b) Intermediate liquid fraction: contact between bubbles along very elongated surfaces. (c) Dry limit. The estimation of the film height ε compared to the Hele-Shaw cell height h is given in the text.

Modelisation of the film shape. – When a single bubble in water is squeezed between two plates separated by a distance h, the gas pressure increases in the bubble. This pressure can be roughly estimated if the air/water interface is approximated by a piece of torus of minor radius $h/2$ and major radius $R-h/2$, R being the radius of the bubble, seen from above (see fig. 1a). As a torus does not have a constant mean curvature, it is not the exact shape taken by the bubble, but if $R \gg h$ this approximation is justified and it will allow us to make simple estimations. The mean curvature determined in the plane $y=0$ between the two plates (the equatorial plane) is $2/h + 1/R$, so the pressure difference between air and water scales like $\Delta P \approx \gamma(2/h + 1/R)$. If another bubble comes into contact, a thin film is created between the bubbles. At this point we assume that every bubble has the same internal pressure, so the thin film is flat. At point A in fig. 1b, one principal curvature vanishes, while the other is $2/(h-\varepsilon)$, with ε the height of the thin film between the bubbles. At point B the two principal curvatures are approximately $2/h$ and $1/R_b$, with R_b the radius of the vertical Plateau border (in the equatorial plane). The disjoining pressure is negligible at these two points, so the pressures must be equal, which leads

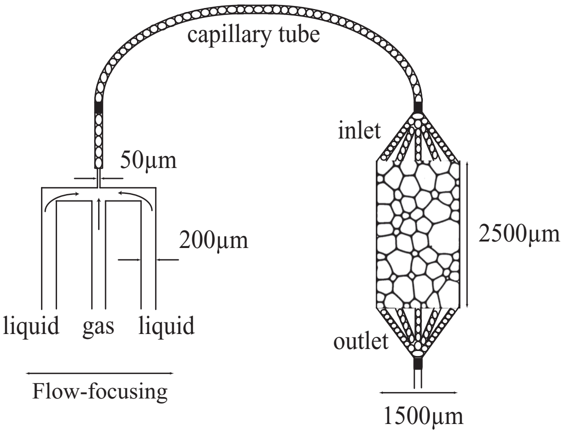

Fig. 2: Scheme of the experimental set-up including the foam generation part and the observation part.

to $2/(h-\varepsilon)=2/(h+1/R_b)$. At first order in ε, it leads to $\varepsilon/h=h/(2R_b)$. Finally, as long as $h \ll R_b$, the bubbles are in contact only along lines of negligible thickness with respect to the channel height. When the liquid fraction decreases and bubbles come even closer to each others, the usual structure of a macroscopic 2D foam is recovered and the vertical and horizontal Plateau borders have the same shape. They have a single non-vanishing principal radius, smaller than h (fig. 1c).

von Neumann's law has been established for this third case.

Let us now consider the case in which two bubbles touch each other along a line instead of a thin film (fig. 1b). Gas diffusion from a bubble 1 to a bubble 2 will occur if this contact line is curved toward bubble 1. In this case, the pressures are indeed $P_1=P_s+\gamma(2/h+1/R_l)$ and $P_2=P_s+\gamma(2/h-1/R_l)$, with P_s the solution pressure, R_l the contact line curvature and P_1 and P_2 the pressure in the two bubbles. The driving force for the gas diffusion is then $\Delta P=2\gamma/R_l$. This relation is identical to the equation obtained in the presence of thin films between the bubbles. Nevertheless the diffusion coefficient, which *a priori* depends on both the film thickness and its height may be very different from the one measured in a macroscopic 2D experiment where the average thickness of the film is much larger with a relative height over the Plateau border also larger than in a 40 μm cell height. It will be shown in the following that the diffusion coefficient we measure is indeed smaller than the values found in the literature.

Experimental set-up. – Flow focusing: microfoams start to be largely studied in microsystems. The traditional way to produce *in situ* two-phase flows in microsystems consists in using a flow-focusing geometry [14]. This geometry is shown in fig. 2. It is composed of a cross-channel intersection, in which the continuous phase enters from each side of the dispersed phase inlet. Garstecki *et al.* [8] showed that the dispersity of bubble sizes generated by this procedure can be controlled by different flow rates of liquid and gas. As coarsening in monodisperse foams exhibits a very specific behavior, we will focus on a relatively polydisperse foam for this study. The PDMS device is composed of an inlet channel (constituted of two embranchments) for the liquid and another one for the gas, both ending near an orifice (smaller than the two inlets channel width $=50\,\mu$m). At the entrance of the orifice the liquid and gas phases form an interface and the pressure drop along the longitudinal axis of the device forces the tip of the gas stream into the orifice. The tip proceeds through the orifice and chases the liquid in the capillary tube. In the orifice, because of the hydrophilic character of the walls (PDMS) the gaseous thread is surrounded by liquid and due to energetics instability, the thread breaks and releases a bubble into the outlet channel. The procedure to manufacture soft lithography microsystem is detailed in [15]. It roughly consists in a PDMS block (transparent polymer), containing the microfluidic circuit. First, a mould is manufactured in a negative photosensible resin (Su-8 2100) and then an imprint is realized in a polymer (PolyDiMethylSiloxane, PDMS RTV 615) which is finally glued on a PDMS surface thanks to a plasma cleaner, thus every wall of the system is in PDMS. The channel height is $h=40\,\mu$m, and the width is either $w=100$ or $200\,\mu$m. The continuous liquid phase is composed of deionized water (93.86%, in mass), glycerol (5.86%) and an anionic surfactant (SDS 0.27%). The surfactant concentration is thus 0.009 mol/L, which is just above the critical micellar concentration —cmc— (0.008 mol/L). The surface tension of the solution was measured by the pendant drop technique and found to be 36 mN/m at 20 °C. Different syringes were used to push the liquid: Terumo (2 and 5 mL) and Upchurch (500 μL). The dispersed gas phase is compressed air and the pressure is controlled by a SMC regulator. This geometry produces flowing foam. Indeed, even if the experimentalist shut all the valves off, the foam keeps moving due to the upstream gas decompression. For this reason, the device is divided into two parts: i) foam production (containing the flow focusing), ii) foam storage (observation room). After production, the foam is thus led into a microtank (reservoir: $1500\times2500\,\mu$m) using a tygon tubing (50 μm). Once the observation room is filled by foam, the tygon tubing is disconnected so that the foam can be isolated and can be observed with a Leica microscope (DMIRB) and a CCD camera (COHU, 25 Hz). Images are stored using NIH image, binarised (ImageJ) and are further processed using Aphelion software. It is possible, using this software, to measure the individual bubbles area as well as their number of faces (number of neighbors) on successive images or to discern internal from peripheral bubbles. Figure 3 shows a typical ageing foam at the beginning of its evolution (a) and at later stages.

Results: typical time for foam ageing. – Figure 4 concerns the total number of internal bubbles $N(t)$.

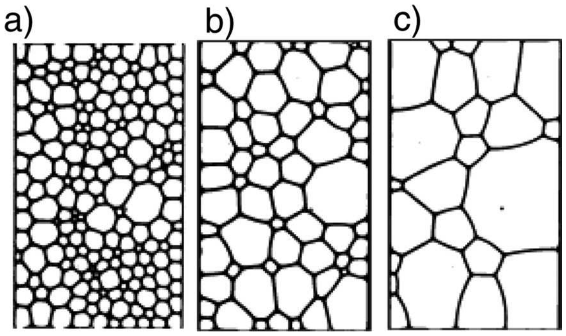

Fig. 3: (a) Initially 190 bubbles, (b) 66 bubbles remaining after $\Delta t(a \to b) = 10'$, (c) 23 bubbles remaining after $\Delta t(a \to c) = 30'$.

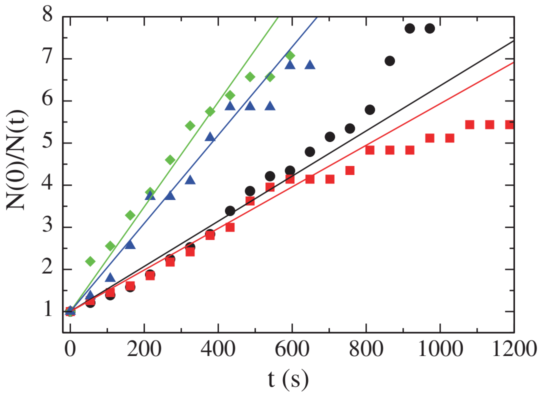

Fig. 4: Number of internal bubbles as a function of time. A characteristic time can be defined for both populations of bubbles.

We plotted $N(0)/N(t)$ as a function of time for four different experiments. This law is expected to be linear in a scale-invariant regime [16], if the effective diffusion coefficient is constant, which is observed experimentally, before boundary effects become non-negligible. This is in good agreement with the fact that the Plateau border size observed on the images is constant since the liquid can be exchanged with an external reservoir. We are thus confident that this coefficient is constant.

Several effective diffusion coefficient lead to various slopes, probably corresponding to slightly different liquid fractions, as discussed in the conclusion. From these curves we extract two characteristic times: i) the time for which half of the bubbles have disappeared, which we define as an order of magnitude of a characteristic time for practical issues in a standard situation (thickness of microfluidic system, size of storing chamber). This time is found to be around 2 or 3 minutes, but polydispersity is much more higher than other microfoams [8,9]. ii) The time after which we cannot extract pertinent information, due to a lack of statistics and due to boundary effects. This time, around 10 minutes, is characterised by the departure from the linear law in fig. 4.

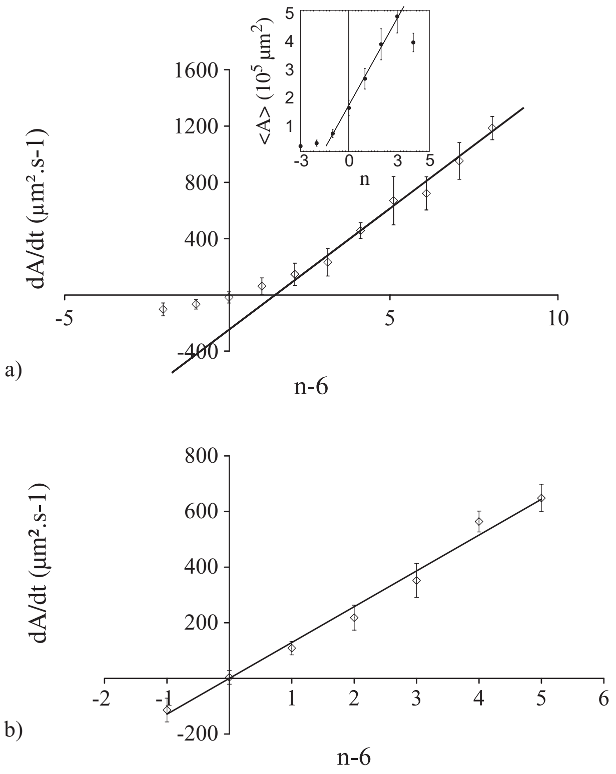

Fig. 5: dA/dt as a function of $n-6$ for a) all internal bubbles, b) large internal bubbles. The inset is the Lewis law: mean area of n-sided bubbles as a function of n.

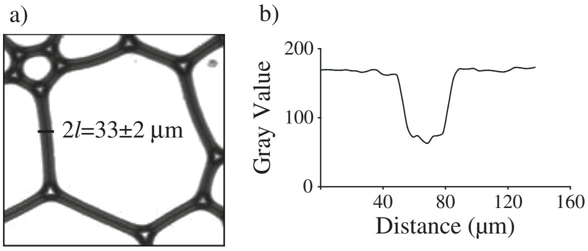

Fig. 6: a) Estimation of the curvature radius at the Plateau borders and b) the length l is half-thickness at the minimum of the Gray level.

Results: von Neumann's law. – We now turn to von Neumann's law (eq. (1)). Figure 5 is a scatter plot of dA/dt as a function of neighbors $n-6$, followed during ageing process. This plot is an average on all inner bubbles, for four different experiments. It is noticeable that there is a departure from the linear law at small face number. This variation is easily understood; indeed, almost all smallest bubbles circumference is part of Plateau borders, where the foam is locally wetter (see fig. 6a), thus leading to a smaller diffusion coefficient. The mean area of n-sided bubbles follows a linear fit as a function of n as shown in the inlet of fig. 5a. The discrepancy at large n is due to a lack of statistics (bounded foam), while the discrepancy at small n is due to the presence of Plateau borders (higher liquid fraction). In order to measure the diffusion coefficient corresponding to bubble edges and to check the validity of von Neumann's law, we plot in fig. 5b the evolution of $\mathrm{d}A/\mathrm{d}t = f(n-6)$ for larger bubbles (of area larger than the mean area), *i.e.* for dryer bubbles. Since $\mathrm{d}A/\mathrm{d}t$ *vs.* n is linear, von Neumann's law is valid in microfoam, and the statistical analysis gives a diffusion coefficient $D_{\text{eff}} = 128\,\mu\text{m}^2 \cdot \text{s}^{-1}$. This value is one order of magnitude smaller than the coefficient measured by Princen for similar solutions [10]. This discrepancy arises from geometrical effects that are detailed in the next section.

In order to explain this discrepancy, Glazier and Stavans [7,17] introduced a correction to von Neumann's law which takes into account the fact that angles at the Plateau borders junction can deviate from 120° (taking into account additional non-linear curvature energy), and the corresponding angle depends on the number of neighbors of the bubble. However, another explanation arises from Weaire [18] who proposed that the finite size of the Plateau border is responsible for this discrepancy. As we recover a linear regime on fig. 5 by keeping only the larger bubbles, we believe that this second explanation is in better agreement with the experimental results, which thus provide here a possible experimental answer to an old controversy.

Liquid film height and thickness —determination of film shape by image analysis. – The light intensity profile across the Plateau border (see fig. 6) exhibits a sharp transition between two Gray levels, allowing us to extract a well-defined characteristic length $l = 17 \pm 2\,\mu$m (see fig. 6), which is invariant with time. The relation between r and l depends in a complex way on the light refraction by the gas/fluid interface, but if l is constant with time, then r is constant too. This allows us to conclude with a good precision that Plateau borders have a constant size during the experiments. A quantitative image processing can be performed in order to deduce r from a measurement of l [19], but only with pictures of higher resolution.

The extracted length can thus be only considered as the order of magnitude of the Plateau border radius, leading to $r \sim 10$–$30\,\mu$m. This is compatible with the channel thickness but does not enable us to conclude whether the adjacent bubbles are in contact along a line or along a thin film (see fig. 1). However, even with an improved optical set-up, it would probably be difficult to predict the height ε of the thin film, which, if present, is very small. It will be deduced indirectly from the diffusion coefficient measurements.

From the estimation of the Plateau border radius, we deduce an estimation of disjoining pressure, which is $\Pi_d = 2\gamma/r \sim 4.5\,10^3$ Pa in our case. The film thickness is thus $e_0 = 16$ nm [20,21], corresponding to the first common black film.

Diffusion coefficient for any liquid phase shape. – In this section, the diffusion coefficient D_{eff} is determined theoretically as a function of the film shape for the geometry of fig. 1b and compared to the diffusion coefficient of a thin film of constant thickness e.

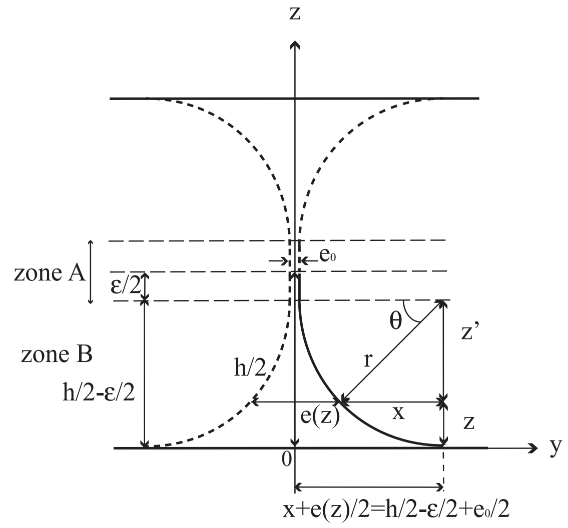

Fig. 7: Parametrisation of liquid phase shape for the calculation of D_{eff}.

From eq. (2), applied to a variable film thickness, we get[1]

$$D_{\text{eff}} = \frac{2\pi\gamma}{3\,P_0}\,\frac{1}{h}\int_0^h k(z)\,\mathrm{d}z. \qquad (4)$$

The integral factor contains the information on the shape of the film. Princen and Mason derived the following expression for the permeability k of an e-thick liquid film:

$$k(z) = \frac{D_w\,H}{e(z) + 2\,h_{ML}}, \qquad (5)$$

where h_{ML} is the effective thickness of an interface ($\sim 1\,\text{Å}$), $D_w \sim 2 \cdot 10^{-9}\,\text{m}^2/\text{s}$ is the gas diffusion constant inside the liquid, and $H \sim 1.6 \cdot 10^{-2}$ is the gas concentration ratio between the gas and the fluid phases, *i.e.* $HP/(RT) = C$, with C the concentration of gas in the fluid phase.

For a film of constant thickness e, D_{eff} is thus

$$D_{\text{eff}} = \frac{2\pi\gamma}{3\,P_0}\,\frac{D_w\,H}{e + 2\,h_{ML}}. \qquad (6)$$

Let us now consider the situation of fig. 7, in which there are two regions: one is a film of height ε and thickness e_0, and a second region is a film of non-constant thickness $e(z)$. Considering the parameterization given in fig. 7, the thickness at height z is

$$e(z) = e_0 + (h-\varepsilon) - \sqrt{(h-\varepsilon)^2 - (h-\varepsilon-2\,z)^2}, \qquad (7)$$

$$\text{for} \qquad 0 < z < \frac{h-\varepsilon}{2}$$

---

[1] Indeed this is an approximation: we assume that the gradient of concentration is perpendicular to the film interfaces. This approximation is easy to justify in the case of a slowly varying thickness.

and

$$e(z) = e_0, \qquad \text{for} \qquad \frac{h-\varepsilon}{2} < z < \frac{h}{2}. \tag{8}$$

Since we may assume that $e_0 \gg h_{ML}$, this leads to

$$D_{\text{eff}} = \frac{2\pi\gamma}{3}\,\frac{D_w\,H}{P_0}\,\frac{2}{h}\left[\int_0^{(h-\varepsilon)/2} \frac{1}{e(z)}\,\mathrm{d}z + \int_{(h-\varepsilon)/2}^{h/2} \frac{1}{e_0}\,\mathrm{d}z\right]. \tag{9}$$

This integral is expanded using the small parameter $e_0/(h-\varepsilon)$ leading to the result:

$$D_{\text{eff}} = \frac{2\pi\gamma}{3}\,\frac{D_w\,H}{h\,P_0}\left(\pi\sqrt{\frac{h-\varepsilon}{2\,e_0}} + \frac{\varepsilon}{e_0}\right). \tag{10}$$

The influence of both terms, arising, respectively, from the Plateau borders and from the thin film, depends on ε. With $h{=}40\cdot 10^{-6}\,\text{m}$, $P_0{=}10^5\,\text{Pa}$, $D_{\text{eff}}{=}128\cdot 10^{-12}\,\text{m}^2\cdot\text{s}^{-1}$, $\gamma = 36\cdot 10^{-3}\,\text{N}\cdot\text{s}^{-1}$, $D_w = 2\cdot 10^{-9}\,\text{m}^2\cdot\text{s}^{-1}$ and $H = 1.6\cdot 10^{-2}$, we get, assuming the thin film is a common black film and $e_0 = 16\cdot 10^{-9}\,\text{m}$,

$$\varepsilon \sim 10^{-1} h. \tag{11}$$

In this case, the largest part of the gas diffusion occurs through the thin film. This is the case as long as $\varepsilon \gg \sqrt{h e_0}$. The permeability coefficient k (see eq. (3)) is usually measured on a single bubble trapped below a liquid/gas interface by monitoring the radius decrease [10]. In this situation, the disjoining pressure is of the order of γ/l_c, with l_c the capillary length, so $\Pi_d \sim 10\,\text{Pa}$. For this pressure, the thin film may be in a relatively thick metastable state (typically $e_0 \sim 30\,\text{nm}$ [21]).

In our situation, the height of the thin film is much smaller than the foam thickness, which reduces the effective diffusion coefficient (here by a factor 10). In contrast, the film thickness is reduced by a factor 2. According to the Princen model, this increases D_{eff}.

Conclusion. – This work was motivated by two main questions: i) From an applicative side: is it possible to store gas pockets in a microfluidic system? ii) From fundamental interests: does a foam confined in a microcell behaves following traditional constitutive laws? To answer the first question, we were able to extract a typical time of foam ageing of about 2–3 mn for polydispersed foam. This means that storing gas pocket should not exceed this typical time for practical applications, at least for a polydisperse foam; considering that the typical time increases while decreasing polydispersity.

To answer the second question, we found that D_{eff} is one order of magnitude smaller than the one found in 2D macrofoam coarsening. The estimation of the radius of curvature allows to estimate the film thickness being two times smaller than the usual 2D macrofoam. Furthermore, a calculation providing the contribution of gas diffusion from either a thin-film thickness or a non-constant film thickness shows that most diffusion occurs through the thin film as expected. We finally came to the conclusion that the film height is about one tenth of the channel height.

***

The authors wish to thank CNRS, ENS-Cachan and Rennes Metropole for financial support.

REFERENCES

[1] Shin Y. S., Cho K., Lim S. H., Chung S., Park S. J., Chung C., Han D. C. and Chang J. K., *J. Micromech. Microeng.*, **13** (2003) 768.

[2] Huang B., Wu H., Kim S. and Zare R. N., *Lab Chip*, **5** (2005) 1005.

[3] Durian D. J., Weitz D. A. and Pine D. J., *Science*, **252** (1991) 686.

[4] Ganàn-Calvo A. M., Fernàndez J. M., Marquez Oliver A. and Marquez M., *Appl. Phys. Lett.*, **84** (2004) 4989.

[5] Glazier J. A. and Weaire D., *J. Phys: Condens. Matter*, **4** (1992) 1867.

[6] von Neumann J., *Metal Interfaces* (American Society of Metals, Cleveland) 1952, p. 108.

[7] Glazier J. A. and Stavans J., *Phys. Rev. A*, **40** (1989) 7398.

[8] Garstecki P., Gitlin I., DiLuzio W., Whitesides G. M., Kumacheva E. and Stone H. A., *Appl. Phys. Lett.*, **85** (2004) 2649.

[9] Raven J.-P., Marmottant P. and Graner F., *Eur. Phys. J. B*, **51** (2006) 137.

[10] Princen H. M., Overbeek J. Th. G. and Mason S. G., *J. Colloid Interface Sci.*, **24** (1967) 125.

[11] Glazier J. A., Gross S. P. and Stavans J., *Phys. Rev. A*, **36** (1987) 306.

[12] Rosa M. E. and Fortes M. A., *Philos. Mag. A*, **79** (1999) 1871.

[13] Stavans J., *Phys. Rev. A*, **42** (1990) 5049.

[14] Ganàn-Calvo A. M. and Gordillo J. M., *Phys. Rev. Lett.*, **87** (2001) 274501.

[15] Xia Y. and Whitesides G. M., *Angew. Chem., Int. Ed.*, **37** (1998) 550.

[16] Stavans J., *Rep. Prog. Phys.*, **56** (1993) 733.

[17] Stavans J. and Glazier J. A., *Phys. Rev. Lett.*, **62** (1989) 1318.

[18] Weaire D., *Phys. Rev. Lett.*, **64** (1990) 3202.

[19] van der Net A., Blondel L., Saugey A. and Drenckhan W., *Colloids Surf.*, **309** (2007) 159.

[20] Mysels K. J. and Jones M. N., *Discuss. Faraday Soc.*, **42** (1966) 42.

[21] Bergeron V. and Radke C. J., *Langmuir*, **8** (1992) 3020.